The Astrophysical Journal Letters, 827:L40 (8pp), 2016 August 20 doi:10.3847/2041-8205/827/2/L40

A SEARCH FOR AN OPTICAL COUNTERPART TO THE GRAVITATIONAL-WAVE EVENT GW151226

S. J. Smartt[1], K. C. Chambers[2], K. W. Smith[1], M. E. Huber[2], D. R. Young[1], T.-W. Chen[3], C. Inserra[1], D. E. Wright[1], M. Coughlin[4], L. Denneau[2], H. Flewelling[2], A. Heinze[2], A. Jerkstrand[1], E. A. Magnier[2], K. Maguire[1], B. Mueller[1], A. Rest[5], A. Sherstyuk[2], B. Stalder[2], A. S. B. Schultz[2], C. W. Stubbs[3], J. Tonry[2], C. Waters[2], R. J. Wainscoat[2], M. Della Valle[6,7], M. Dennefeld[8], G. Dimitriadis[9], R. E. Firth[9], M. Fraser[10], C. Frohmaier[9], A. Gal-Yam[11], J. Harmanen[12], E. Kankare[1], R. Kotak[1], M. Kromer[13], I. Mandel[14], J. Sollerman[13], B. Gibson[2], N. Primak[2], and M. Willman[2]

[1] Astrophysics Research Centre, School of Mathematics and Physics, Queens University Belfast, Belfast BT7 1NN, UK; s.smartt@qub.ac.uk
[2] Institute of Astronomy, University of Hawaii, 2680 Woodlawn Drive, Honolulu, HI 96822, USA
[3] Max-Planck-Institut für Extraterrestrische Physik, Giessenbachstraße 1, D-85748, Garching, Germany
[4] Department of Physics, Harvard University, Cambridge, MA 02138, USA
[5] Space Telescope Science Institute, 3700 San Martin Drive, Baltimore, MD 21218, USA
[6] INAF, Osservatorio Astronomico di Capodimonte, Salita Moiariello 16, I-80131, Napoli, Italy
[7] ICRANET, Piazza della Repubblica 10, I-65122, Pescara, Italy
[8] Institut d'Astrophysique de Paris, CNRS, and Universite Pierre et Marie Curie, 98 bis Boulevard Arago, F-75014, Paris, France
[9] School of Physics and Astronomy, University of Southampton, Southampton, SO17 1BJ, UK
[10] Institute of Astronomy, University of Cambridge, Madingley Road, Cambridge, CB3 0HA, UK
[11] Benoziyo Center for Astrophysics, Weizmann Institute of Science, 76100 Rehovot, Israel
[12] Tuorla Observatory, Department of Physics and Astronomy, University of Turku, Väisäläntie 20, FI-21500 Piikkiö, Finland
[13] Department of Astronomy and the Oskar Klein Centre, Stockholm University, AlbaNova, SE-106 91 Stockholm, Sweden
[14] School of Physics and Astronomy, University of Birmingham, Birmingham B15 2TT, UK
Received 2016 June 6; revised 2016 August 5; accepted 2016 August 7; published 2016 August 19

ABSTRACT

We present a search for an electromagnetic counterpart of the gravitational-wave source GW151226. Using the Pan-STARRS1 telescope we mapped out 290 square degrees in the optical i_{P1} filter, starting 11.5 hr after the LIGO information release and lasting for an additional 28 days. The first observations started 49.5 hr after the time of the GW151226 detection. We typically reached sensitivity limits of $i_{P1} = 20.3$–20.8 and covered 26.5% of the LIGO probability skymap. We supplemented this with ATLAS survey data, reaching 31% of the probability region to shallower depths of $m \simeq 19$. We found 49 extragalactic transients (that are not obviously active galactic nuclei), including a faint transient in a galaxy at 7 Mpc (a luminous blue variable outburst) plus a rapidly decaying M-dwarf flare. Spectral classification of 20 other transient events showed them all to be supernovae. We found an unusual transient, PS15dpn, with an explosion date temporally coincident with GW151226, that evolved into a type Ibn supernova. The redshift of the transient is secure at $z = 0.1747 \pm 0.0001$ and we find it unlikely to be linked, since the luminosity distance has a negligible probability of being consistent with that of GW151226. In the 290 square degrees surveyed we therefore do not find a likely counterpart. However we show that our survey strategy would be sensitive to NS–NS mergers producing kilonovae at $D_L \lesssim 100$ Mpc, which is promising for future LIGO/Virgo searches.

Key words: gravitational waves – supernovae: general – surveys

1. INTRODUCTION

The Advanced LIGO experiment detected the first transient gravitational-wave signal (GW150914) from the inspiral and merger of a pair of black holes of masses $36\,M_\odot$ and $29\,M_\odot$ (Abbott et al. 2016d). This was remarkable not only for being the first direct detection of gravitational waves but the first evidence that binary black holes (BBH) exist, and the largest mass estimates for black holes in the stellar regime (Abbott et al. 2016a). This has been followed by a second discovery, also of a BBH merger signal, with a pair of black holes with masses $14.2^{+8.3}_{-3.7} M_\odot$ and $7.5^{+2.3}_{-2.3}\ M_\odot$ (Abbott et al. 2016b) on 2015 December 26 (GW151226). LIGO estimates a luminosity distance of 440^{+180}_{-190} Mpc, corresponding to a redshift $z = 0.09^{+0.03}_{-0.04}$ (90% limits).[15]

A broad range of teams have begun efforts to follow-up GW signals to detect the putative electromagnetic (EM) counterparts. The first event resulted in 25 teams of observers covering the LIGO sky localization region with gamma-ray to radio facilities (summarized in Abbott et al. 2016c). The general assumption has been that BBH mergers will not produce a detectable EM signature. However, *Fermi* may have detected a weak X-ray transient that was temporally coincident with GW150914 (Connaughton et al. 2016), although the reality of the detection is disputed by Greiner et al. (2016). Loeb (2016) suggested a novel mechanism that may produce both a BBH merger and a relativistic jet from the fragmentation of a rapidly rotating core of a single massive star. However, if the *Fermi* hard X-ray detection is real, it is more like a short gamma-ray burst than a long one. Furthermore, Woosley (2016) investigated this scenario quantitatively and found a single star origin to be unlikely. Perna et al. (2016) proposed a short GRB may be formed if the two black holes are formed within a fossil disk that restarts accretion due to tidal forces and shocks during the BBH merger. Hence the searches continue, particularly as a detection would open up a major new way to probe high-energy astrophysics, stellar evolution, compact remnants, and test modified theories of gravity (Lombriser & Taylor 2016).

[15] Throughout, we adopt the same cosmological parameters as Abbott et al. (2016b) of $H_0 = 69$ km s^{-1}, $\Omega_M = 0.31$, $\Omega_\Lambda = 0.69$.

Here we present the results of our wide-field search for an optical counterpart to the transient gravitational-wave event GW151226 using the Pan-STARRS1 (PS1) and the ATLAS survey telescopes combined with spectroscopic follow-up from Hawaiian facilities and the Public ESO Spectroscopic Survey of Transient Objects (PESSTO).

2. OBSERVING CAMPAIGN OF SOURCE GW151226

To search for optical counterparts to gravitational-wave events our collaboration (Smartt et al. 2016) uses the PS1 system (Kaiser et al. 2010) for imaging and relies on the existence of the PS1 3π Survey (K. Chambers et. al. 2016, in preparation) for template images. The PESSTO Survey (Smartt et al. 2015), together with programs on Gemini North with GMOS and the UH2.2 m with SNIFS, provides spectroscopic classification. The data for one object discovered here were supplemented with *Hubble Space Telescope* (*HST*) observations. GW151226 was detected on 2015 December 26 03:39 UTC (MJD 57382.152) and released to the EM community as a discovery on 2015 December 27 17:40 UTC (Abbott et al. 2016b). The initial localization generated by the BAYESTAR pipeline (Singer & Price 2016) contained a 50% credible region of 430 square degrees and a 90% region of about 1400 square degrees (to be compared with a 90% credible region of 630 square degrees for GW150914 Abbott et al. 2016c). We began taking data with the PS1 telescope during the next available dark hours, on 2015 December 28 05:08 UTC (11.47 hr after the LIGO information release and 49.48 hr after the event time) and mapped out a region of 214 square degrees on this first night as shown in Figure 1.

The same region was mapped on the two subsequent nights (extending to 273 square degrees). All observations were done with the PS1 $i_{\rm P1}$ filter with a four-point dither pattern at each pointing center. The four individual (back to back) 45 s exposures were co-added to produce a 180 s exposure and the PS1 3π $i_{\rm P1}$ reference image (typically having an effective total exposure time of 270–900 s) was subtracted from this 180 s night stack (see E. Magnier et al. 2016, in preparation and Smartt et al. 2016, for more details). On any one night this 180 s exposure sequence was repeated multiple times (2–3) in the central highest probability region, giving us some intra-night sampling. The sequence was repeated an additional five times between 2016 January 02 and January 25 (extending the full footprint to a total of 290 square degrees). The observing cadence and sensitivity are illustrated in Figure 1, and the full PS1 footprint corresponds to 26.5% of the full LIGO posterior probability. This footprint choice was a combination of the telescope accessibility of the LIGO localization map and a choice to go deeper on the higher probability regions (Coughlin & Stubbs 2016).

We selected targets with similar filtering algorithms as described in our first paper (Smartt et al. 2016). A total of 2.3×10^7 detections were ingested into the database (after basic rejections of known defects). Spatial aggregations of detections within 0.″5 of each other resulted in the creation of 1.1×10^7 objects and basic filtering and the insistence of two separate detections resulted in a total of 1.7×10^6 candidate astrophysical transients. Subsequent filtering (obvious dipoles, stellar objects, and objects near bright stars) and a random forest machine learning classifier reduced the numbers to 144,000 for which the pixel recognition machine learning technique was employed (Wright et al. 2015; Smartt et al. 2016). Further removal of 3903 known minor planets left a total of 24,100 objects for humans to scan and this manual process resulted in 85 objects for further investigation. The human scanning involved removing artifacts that are obvious to the eye but that are not properly recognized by the machine learning. As we wanted to err on the side of completion over purity, we set the machine learning threshold to roughly a 20% false positive rate on the ROC curve (see Figure 7 of Wright et al. 2015, for an illustration). The human scanning removed subtraction and chip defects that are easily distinguished visually. We note that in the Milky Way plane there were at least an additional 43 faint transients that are very likely variable stars that reach above our detection limit on a few epochs. A few could be background hostless supernovae, but their location in the plane suggests they are faint stellar variables.

In addition, the ATLAS 0.5 m telescope (Tonry 2011) covered a significant fraction of the northern sky in the first five days after GW151226 as shown in Figure 1. These data were taken during normal ATLAS operations and can be thought of as ATLAS working in serendipitous mode. In the future, ATLAS will be able to work in targeted mode in the same way as PS1. A single ATLAS unit, with its 30 square degree cameras, can map out 1000 square degrees within 30 minutes. We highlight that just 3 hr after the GW151226 event detection, ATLAS serendipitously covered 87 square degrees of the sky localization region (2.2% enclosed probability) during the time window 57382.302 ± 0.014. We processed all ATLAS data taken serendipitously in the first five days to locate transients as in Tonry et al. (2016). After processing about 575 square degrees, the ATLAS coverage increases the total enclosed probability to 36% over the first five days from GW151226, getting to median 5σ limits of $m_o \simeq 19.0$ (orange filter). Apart from variable stars and CV candidates, we found no other extragalactic transient candidates in this stream.

2.1. Discovery and Spectroscopic Classification of Transients

During our filtering, we removed obvious Galactic stellar variables and known active galactic nucleus candidates. After removing these contaminants, we found 49 transients that are either confirmed SNe or likely SNe, which are all summarized in Table 1. As discussed in Smartt et al. (2016) the detected transients are dominated by mostly old supernovae that exploded over an extended period before the GW trigger. The sky positions of transients found in the first three days are plotted in Figure 1. Those with spectroscopic classifications are listed along with their redshifts. We suggest that all these objects are unrelated field supernovae, although one object, PS15dpn, deserves closer inspection and is discussed in the next section.

We note two objects that are unrelated to GW151226 but are worth highlighting in the context of searching for unusual transients in LIGO/Virgo sky localization regions. PS15dqa is a faint transient in the nearby ($D = 7$ Mpc) galaxy NGC 1156. The transient magnitude $i_{\rm P1} = 20.8$ implies $M_i = -8.9$ (including significant Milky Way foreground extinction of $A_i = 0.36$). An *HST* archive image with the Advanced Camera for Surveys (in filter F625W) of NGC 1156 shows an object that is astrometrically coincident with PS15dqa to within 0.″3. This is a stellar point source with $m_{\rm F625W} = 20.1$ and hence $M_r = -9.6$. Assuming a bolometric correction of zero, this corresponds to $\log L/L_\odot = 5.7$ dex, which implies a 50–60 $M_\odot$

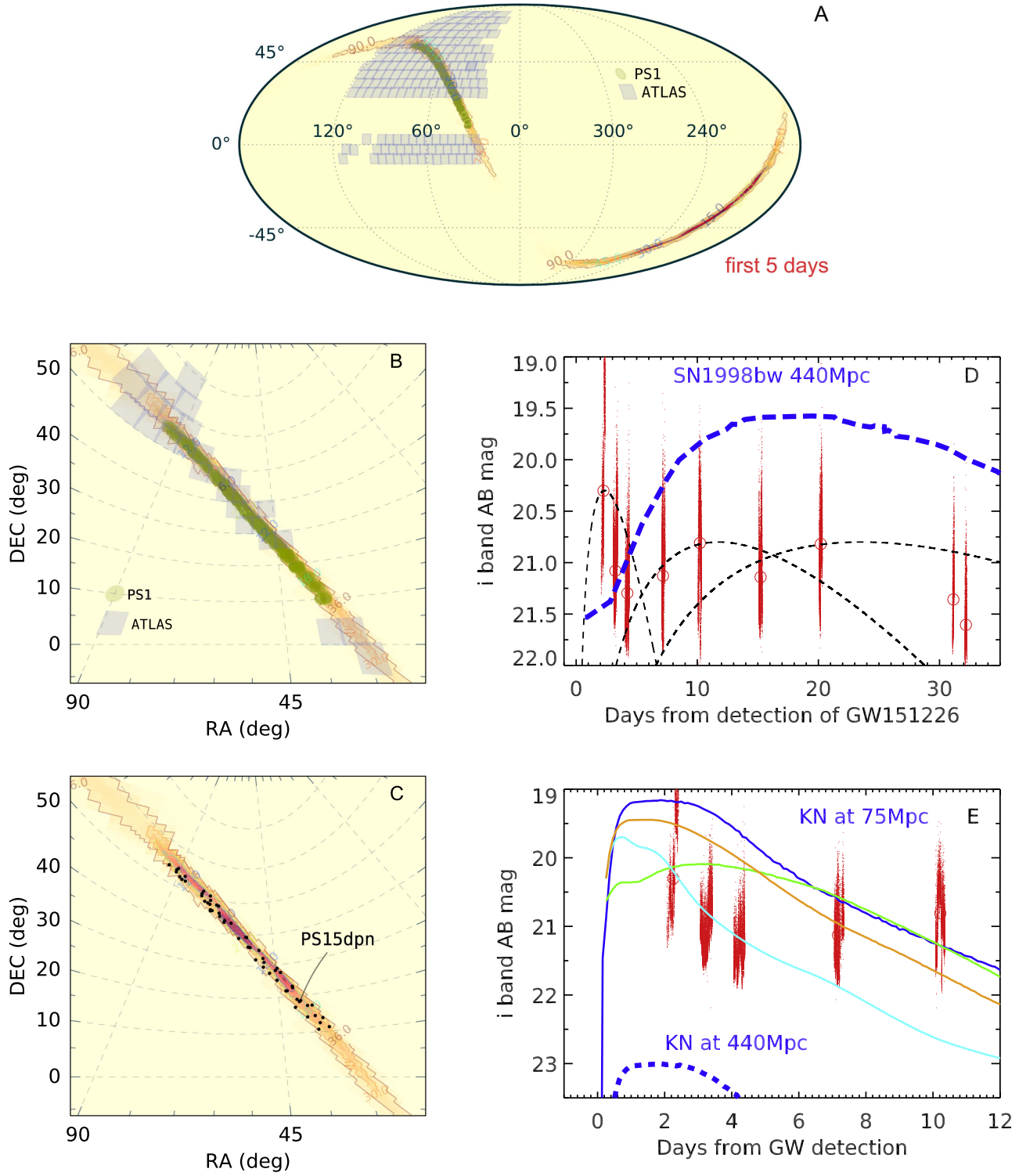

Figure 1. A: LIGO sky localization region showing Pan-STARRS1 and ATLAS sky coverage within five days of GW151226. B and C: Zoom-in of our focused region with Pan-STARRS1 and ATLAS sky coverage with transients detected. D: 5σ detection limits for all i_{P1} images, with the median nightly value marked as red open circles. The black curves are parameterized light curves of three different timescales (4d, 20d, 40d) and the blue line is SN1998bw placed at $D_L = 440$ Mpc. E: NS–NS mergers expected to be detected within $D_L = 75$ Mpc, as expected in the upcoming 2016 LIGO-VIRGO run. Our 5σ limits are shown with kilonova models. Blue: the disk wind outflows of compact object mergers of Kasen et al. (2015). Orange: an r-process powered merger model that includes a ^{56}Ni-dominated wind (Barnes & Kasen 2013). Cyan: merger model with iron-group opacity with $M_{ej} = 0.01\ M_\odot$ by the same authors. Green: merger model for opacity dominated by r-process elements, with $M_{ej} = 0.1\ M_\odot$ also by the same authors. All model magnitudes are in SDSS-like *i*-band, AB mags.

star that is undergoing brightness variations by a factor of 2. While this scale of variability is known for massive stars of this luminosity, and is unrelated to GW151226, it illustrates our ability to identify faint transients in nearby galaxies. Second, PS16li is a fast optical transient with a 1.3 magnitude fade in 13 minutes on the night of MJD = 57397.51 with a faint, red

Table 1
Transients Discovered by Pan-STARRS1

Name	R.A. (J2000)	Decl. (J2000)	Disc. MJD[d]	Disc Mag	Spec MJD	Type	Spec z	Classification Source and Notes
PS15dcq	03 22 55.83	+34 59 23.6	57384.29	19.99	57388.92	Ia	0.072	iPTF15fgy, Cenko et al. (2016a), Copperwheat & Steele (2016b)
PS15dov[f]	03 43 57.36	+39 17 43.7	57384.32	19.73	57386.32	II	0.016702	GMOS[a], Chambers et al. (2016)
PS15dot	02 11 55.69	+13 28 17.8	57384.34	20.97	57386.30	II	0.149	GMOS, Chambers et al. (2016)
PS15coh	02 15 58.45	+12 14 13.6	57384.34	17.72	57329.22	Ia	0.020	old SN, ASASSN-15rw, iPTF15fev, Cenko et al. (2016a), Copperwheat & Steele (2016a)
PS15dow	02 19 42.20	+14 09 54.7	57384.34	20.22	57387.21	Ib	0.05	GMOS, Chambers et al. (2016)
PS15csf	02 26 02.24	+17 03 40.4	57384.35	18.68	57335.18	II	0.021	PESSTO[b], old SN ATel#8264
PS15dom	02 34 45.62	+18 20 37.7	57384.35	19.01	57390.	II	0.034	old SN, PSN J02344555+182039, iPTF15fdv Pan et al. (2016)
PS15don	02 37 11.44	+19 03 20.2	57384.35	20.47	57388.20	Ia	0.160	GMOS
PS15doy	02 47 54.16	+21 46 24.0	57384.38	20.75	57388.23	Ia	0.190	GMOS
PS15dox	02 40 15.05	+22 32 12.1	57384.38	19.23	57389.06	Ia	0.080	PESSTO, Frohmaier et al. (2016)
PS15dpq	03 09 12.74	+27 31 16.9	57384.39	18.84	57389.04	Ia	0.038	PESSTO, iPTF15fel, Frohmaier et al. (2016) Copperwheat & Steele (2016a)
PS15dpa	02 57 56.02	+28 53 37.1	57384.40	19.51	57389.03	Ia	0.079	PESSTO, Frohmaier et al. (2016), MASTER OTJ025756.02+285337 Lipunov et al. (2016)
PS15dpl	05 47 45.39	+53 36 32.4	57384.43	19.34	57387.40	Ia	0.03	SN2016J, ASASSN-16ah, Chambers et al. (2016)
PS15dpe	05 44 42.66	+52 24 57.9	57384.43	19.44	57388.25	Ia	0.057	GMOS
PS16ku	02 19 06.15	+10 37 45.5	57385.22	20.95	57401.24	II	0.061	SNIFS
PS15dpn	02 32 59.75	+18 38 07.0	57385.23	20.69	57387.23	Ibn	0.1747	GMOS, Chambers et al. (2016), iPTF15fgl, Cenko et al. (2016b) Palazzi et al. (2016), Castro-Tirado et al. (2016)
PS15doz	02 53 41.68	+27 29 57.8	57385.25	20.69	...	...	...	Likely SN[e], slow rise
PS15dpc	03 55 46.16	+38 52 49.6	57385.27	20.95	57387.26	II	0.056	GMOS, Chambers et al. (2016)
PS15dqc	05 51 13.43	+52 28 18.7	57385.29	21.16	...	...	...	Likely SN
PS15cvo	02 20 37.39	+17 02 17.9	57385.31	20.45	...	...	...	MASTER022037.36+170217.5, old SN
PS15dpz	02 40 33.01	+23 00 10.8	57385.32	21.15	...	...	...	Likely SN
PS15dpb	03 42 23.40	+39 14 40.4	57385.36	20.20	57386.43	II	0.041045	GMOS, Chambers et al. (2016)
PS15dpg	03 17 18.88	+32 20 06.9	57385.41	20.86	...	...	...	Likely SN
PS15dpx	06 04 35.54	+53 35 25.8	57385.56	20.76	57395.48	...	0.051	SNIFS[c], featureless.
PS15dou	06 03 38.73	+54 41 12.1	57385.56	20.20	57395.51	II	0.079	SNIFS, D'Avanzo et al. (2016)
PS15dpu	02 40 41.35	+16 49 52.0	57386.22	17.26	57396.88	II	0.0292	ASASSN-15un, D'Avanzo et al. (2016)
PS15dpt	02 07 34.96	+11 03 25.2	57386.22	20.64	57395.36	...	...	SNIFS, red continuum, possible foreground
PS15dpy	02 28 22.75	+13 59 19.3	57386.22	21.31	57395.39	...	...	SNIFS, red continuum, possible foreground
PS15dqa	02 59 41.20	+25 14 12.2	57386.24	20.93	...	...	0.001251	Likely LBV in NGC 1156
PS16cks	04 22 33.25	+43 36 53.0	57386.31	21.45	...	...	...	Likely SN
PS15dqd	05 56 14.60	+52 51 55.2	57386.37	19.92	...	...	...	Likely hostless SN, 0.6^m fade in 3 days
PS15dqe	06 05 26.88	+54 09 11.3	57386.37	21.51	...	...	...	Likely SN
PS16kv	02 22 53.41	+19 15 49.9	57388.22	21.70	...	...	...	Likely SN, host is SDSS J022253.48+191550.5
PS16kx	02 44 42.28	+22 36 39.5	57389.32	21.81	...	...	...	Likely SN
PS16cld	04 51 13.33	+48 59 21.2	57392.26	21.17	...	...	...	Likely SN
PS16kw	02 35 50.63	+17 33 38.2	57394.22	21.27	...	...	...	Likely SN
PS16ky	03 22 34.61	+30 36 07.1	57397.31	20.89	...	...	...	Likely SN
PS16bpe	02 38 48.30	+22 05 56.4	57397.34	21.56	...	...	...	Likely hostless SN
PS16bpf	02 56 00.56	+24 48 51.8	57397.38	21.83	...	...	...	Likely SN
PS16bpj	03 29 06.15	+35 39 07.5	57397.39	21.82	...	...	...	Likely SN
PS16lj	06 23 09.10	+54 38 20.9	57397.51	20.66	57405.24	...	0.088	SNIFS, blue continuum, $M_i = -17.8$
PS15bpk	02 37 09.56	+22 24 02.4	57402.28	21.33	...	...	...	Old SN
PS16bpg	02 56 40.73	+27 40 12.0	57402.28	20.46	...	...	...	Likely SN, rising
PS16bps	06 04 34.63	+53 35 38.8	57402.39	21.20	...	...	...	Likely SN
PS16bpu[f]	03 43 57.13	+39 17 38.4	57402.42	19.34	...	...	0.016702	Likely SN, offset $2\farcs0$ from position of SN2001I
PS16bpw	03 06 54.05	+28 44 23.2	57413.26	21.53	...	...	...	Likely SN, young
PS16bqa	02 38 57.24	+18 10 40.4	57413.30	21.69	...	...	...	Likely SN
PS16aeo	03 30 46.70	+36 38 23.0	57414.28	19.67	...	...	...	Likely SN
PS16bpz	06 31 15.13	+54 51 52.3	57414.35	20.18	...	...	...	Likely SN
Probably stellar variables or AGN variability								
PS15dpp	03 00 39.86	+28 15 25.4	57384.40	20.63	57395.42	...	...	SDSS J030039.86+281525.4, SNIFS. QSO?
PS15dop	03 17 29.58	+29 34 09.2	57384.40	20.01	...	...	...	Likely AGN activity
PS15dpd	05 09 58.63	+50 47 09.4	57384.44	20.34	...	...	...	Likely stellar

Table 1
(Continued)

Name	R.A. (J2000)	Decl. (J2000)	Disc. MJD[d]	Disc Mag	Spec MJD	Type	Spec z	Classification Source and Notes
PS15dpo	02 59 49.56	+25 10 30.4	57385.25	20.55	...	...	...	AGN
PS16li	06 18 59.16	+55 50 55.4	57397.51	20.18	...	...	...	Likely M-dwarf flare
PS16bpx	03 50 03.36	+37 00 52.1	57414.30	18.82	...	...	...	stellar, CSS100113-035003+370052

Notes.
[a] GMOS denotes classification spectra taken for this project with Gemini North and the GMOS spectrometer, with gratings of either R150 or R400.
[b] PESSTO denotes classification spectra taken for this project with PESSTO, as described in Smartt et al. (2016).
[c] SNIFS denotes classification spectra taken for this project with the SNIFS instrument on the UH2.2 m telescope, as described in Smartt et al. (2016).
[d] MJD for GW151226 is 57382.152
[e] "Likely SN" means that the transient is not coincident with an observed point source, nor is a known stellar or AGN variable, and it does have a candidate host galaxy nearby and a light curve that is consistent with being a normal SN.
[f] PS15dov and PS16bpu exploded in the same galaxy, UGC2836. which also hosted SN2001I and SN2003ih.

point source in the PS1 reference stack. This is an M-dwarf flare (e.g., Berger et al. 2013), which highlights our ability to pick up fast decaying transients.

2.2. *PS15dpn: A Type Ibn Supernova Temporally Coincident with GW151226*

This object was reported early in the campaign as being of interest because of its rising light curve and its very blue spectrum (Chambers et al. 2016). We gathered a multi-color PS1 light curve in $grizy_{\rm P1}$ (Schlafly et al. 2012; Tonry et al. 2012; Magnier et al. 2013) and one epoch of *HST* imaging with WFC3 (see Figures 2 and 3), together with eight epochs of spectra. The redshift of the host galaxy is measured at $z = 0.1747 \pm 0.0001$ ($D_L = 854$ Mpc) from the centroids of the strong host galaxy emission lines of Hα, [N II], and [S II]. Figure 4 shows the evolution of this transient into a type Ibn supernova. These SNe are likely the explosion of Wolf–Rayet stars that are embedded in a He-rich circumstellar medium lost by the progenitor system (Foley et al. 2007; Pastorello et al. 2007, 2008). The GMOS spectrum at +26 days post-peak is typical of this class with He I emission lines. The He I λ5876 Å line has FWHM $= 3000\,{\rm km\,s^{-1}}$.

To estimate the explosion epoch, we used a third order polynomial fit to the first six PS1 $i_{\rm P1}$-band detections to estimate a date of 57380.60 ± 2.45. This is 1.6 ± 2.45 days before the detection of GW151226. The uncertainty is estimated from the usage of different fits (order 2–4) and epochs (4–8). Using the first six epochs and a fourth order fit gives an explosion epoch of 57382.03, exactly coincident with GW151226. There is one type Ibn that has a double-peaked light curve (Gorbikov et al. 2014) and if that were common then this method would not be accurate. We calculated the bolometric light curve after applying suitable *K*-corrections (Inserra et al. 2016). A comparison with the only Ibn with an early discovery and well-measured rise (SN 2010al, Pastorello et al. 2015), shows that the two have very different light curve shapes, and therefore SN 2010al is not a good template to use for dating the explosion. This light curve diversity is a feature of Ibn, likely indicating the diverse masses of the CSM and ejecta that power these transients (Pastorello et al. 2008, 2015). This illustrates that PS15dpn was temporally coincident with GW151226 to within 2.45 days. Another unusual feature of PS15dpn is the detection in the radio by the VLA by Corsi & Palliyaguru (2016), which is quite a luminous 6 GHz detection, similar to the relativistic SN 2009bb (Soderberg et al. 2010).

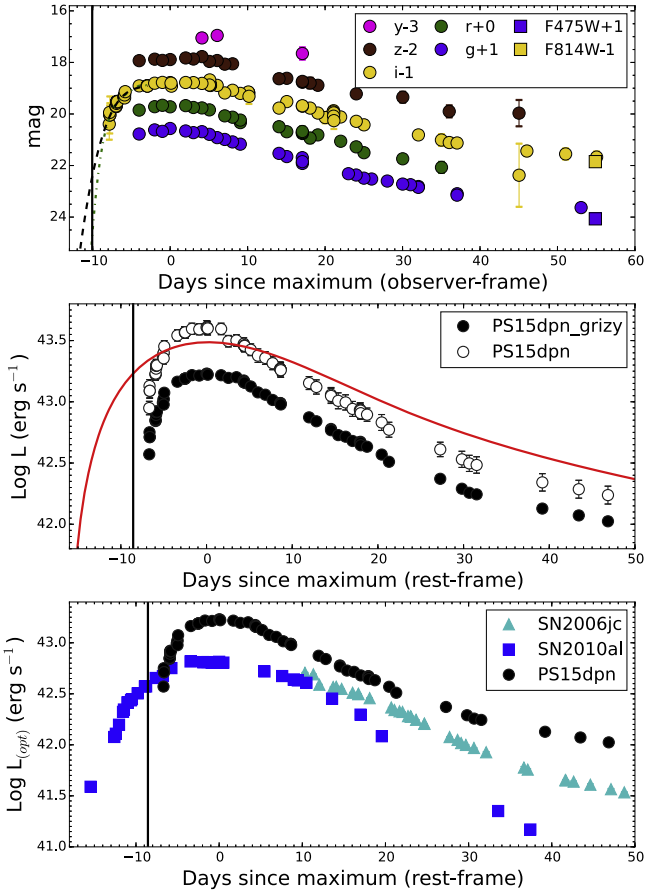

Figure 2. Upper: PS1 light curve of PS15dpn. Circles are PS1 and square symbols are from *HST*. The black dashed line is a third order fit and the green dotted–dashed is a fourth order fit (each fit to the first six epochs). The vertical black line indicates the time of the GW151226 event. Middle: bolometric luminosity calculated with $grizy_{\rm P1}$ filters only (see Inserra et al. 2016 for details) and a full bolometric light curve estimated from a blackbody extrapolation between 0.2 and 2.5 μm. A simple Arnett model, as described in Inserra et al. (2013), is shown for the latter, with input parameters: $E_{\rm exp} = 5 \times 10^{51}$ erg, $M_{\rm ej} = 1.9\,M_{\odot}$, $M_{Ni} = 1.7\,M_{\odot}$. This simply indicates that a ^{56}Ni model is a poor fit and that type Ibn are not well explained by radioactive powering. Lower: comparison with two well observed SN Ibn (Pastorello et al. 2007, 2015).

Therefore PS15dpn caught our attention because of its rarity, and also the fact that the remarkable pre-explosion outburst found for the nearest Ibn (SN2006jc, Pastorello et al. 2007) is still quantitatively unexplained.

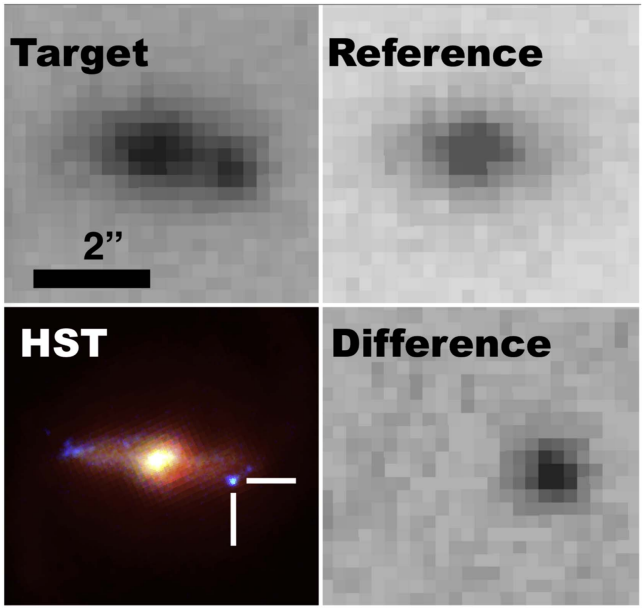

Figure 3. Target, reference, and difference i_{P1} images from PS1 on MJD = 57386 showing PS15dpn offset from its host galaxy; color composite (F475W, F814W, F160W) image from *HST* on MJD = 57447.

Given the temporal coincidence of PS15dpn with GW151226, we estimate the probability of finding a SN Ibn randomly in our sampled field. While we detected PS15dpn at $z = 0.1747$, we would be sensitive to such an object with $M_r \simeq -19.6$ (rest-frame absolute magnitude) to $z = 0.265$. Following the calculations in our first paper (Section 6.3, Smartt et al. 2016), the cosmic rate of core-collapse SNe within $z = 0.265$ implies that within 100 square degrees, there should be 3.1 CCSN explosions per day. We assume an uncertainty in the explosion epoch estimate of PS15dpn of Δt days and a relative rate of Ibn SNe of $\mathcal{R}_{\rm Ibn}$ (which is the fraction of core-collapse SNe that are Ibn). Then the number of Ibn SNe within a survey area of $\mathcal{A}$ square degrees is expected to be

$$N_{\rm Ibn} = 3.1\frac{\mathcal{A}}{100}\mathcal{R}_{\rm Ibn}\Delta t. \quad (1)$$

For $\mathcal{A} = 290$, $\Delta t = 2$, $\mathcal{R}_{\rm Ibn} = 0.01$, this suggests $N_{\rm Ibn} = 0.18$. Hence the probability of a false positive (1 or more events) when the expectation value of 0.18 is simply the Poissonian value $p = 1 - \frac{\lambda^0 e^{-\lambda}}{0!} = 1 - e^{-0.18} = 0.16$. In other words, the probability of finding an unrelated SN Ibn exploding within 2 days of GW151226 that is unrelated and a chance coincidence is $p = 0.16$. This is not convincingly low enough to imply a causal link, but is low enough to highlight that future coincidences should be searched for. One could argue that the appropriate value to use for $\mathcal{R}_{\rm Ibn}$ is significantly less than 0.01, since radio detections at this luminosity for any Ibc SN are quite rare (Soderberg et al. 2010). Alternatively, type Ibc SNe are much more common overall, which would increase the value for $\mathcal{R}_{\rm Ibn}$ significantly. One could speculate that an SN Ibn could potentially be related to a GW source if it were a compact Wolf–Rayet star +BH binary, such as the WR+BH systems in the nearby galaxies IC10 and NGC300 (Prestwich et al. 2007; Crowther et al. 2010). The WR star would need to undergo a core-collapse supernova, followed by a gravitational-wave driven merger with the BH companion within ~2 days. However, assuming that the star was not in contact with the black hole prior to the supernova, the merger would typically require thousands of years rather than days. A very favorable supernova kick toward the BH could reduce the merger timescale, but would require an implausibly high kick velocity and/or a very low-probability kick direction. However, the strongest argument against a link is that the distance estimate to GW151226 is inconsistent with the redshift of PS15dpn (The LIGO Scientific Collaboration and the Virgo Collaboration 2016a). The final probability density function from LIGO drops to zero at $z = 0.1747$ ($D_L = 854$ Mpc), as shown in the detailed companion analysis paper (The LIGO Scientific Collaboration and the Virgo Collaboration 2016b). While the mechanism of Loeb (2016) might predict a rapidly rotating massive star that could conceivably produce both an SN Ibn and GW emission, this now seems unlikely from the calculations of Woosley (2016). Some luminous supernovae have been explained by magnetic NSs born with millisecond periods (Inserra et al. 2013, 2016), and such an object would radiate gravitational waves if it were elliptically deformed. However, an NS origin is excluded, as the LIGO analysis is not consistent with component masses of less than $4.5\,M_\odot$ (99% credible level, Abbott et al. 2016b).

3. DISCUSSION AND CONCLUSIONS

Assuming that none of the transients we found, including PS15dpn, are associated with GW151226, it is useful to set quantitative and meaningful upper limits on potential optical counterparts for BH–BH mergers. These also serve as a guide to our sensitivity to potential future binary neutron star (NS–NS) and neutron star—black hole (NS–BH) merging systems that are more promising systems for producing EM counterparts particularly redward of 7000 Å.

In Figure 1 we show the 5σ limits of every PS1 image taken during this campaign. As described in Smartt et al. (2016), the 5σ limits are calculated for each of the 51 skycells per pointing of the GPC1 camera data products and the median per night is also plotted. We also plot parametrized light curves of three analytic light curves with timescales $t_{\rm FWHM} = 4$, 20, 40 days (as defined in Smartt et al. 2016). These indicate detection limits of $i_{P1} = 20.3$, 20.8, and 20.8, respectively, or $M_i = -18$, -17.5, -17.5 at the luminosity distance of GW151226.

Looking to the future, we plot model light curves of kilonovae from the compact binary mergers (NS–NS) of Kasen et al. (2015) and Barnes & Kasen (2013) as illustrative examples of our survey capability (the merger models of Tanaka & Hotokezaka 2013 and Tanaka et al. 2014 are also of similar luminosity). At the estimated distance of GW151226 of $D_{\rm L} \simeq 440$ Mpc, the predicted fluxes would be very faint (below $i_{P1} \simeq 23$). It is expected that NS–NS mergers will be more common by volume and LIGO's horizon distance for NS–NS detections is a factor of ~5–10 smaller than that for BH–BH mergers, depending on the BH masses (Abadie et al. 2010). During the next science run, beginning in the fall of 2016, LIGO is expected to be sensitive to NS–NS mergers within $D_{\rm L}^{\rm min} \lesssim 75$ Mpc (Martynov et al. 2016) and we show in Figure 1 that our survey strategy would be sensitive to these mergers. Ideally, our goal would be to get 0.5 mag deeper, beginning within 24 hr of the GW alert.

We further show the *i*-band light curve of SN 1998bw (Galama et al. 1998; Patat et al. 2001), which is the typical energetic type Ic SN associated with long-duration gamma-ray

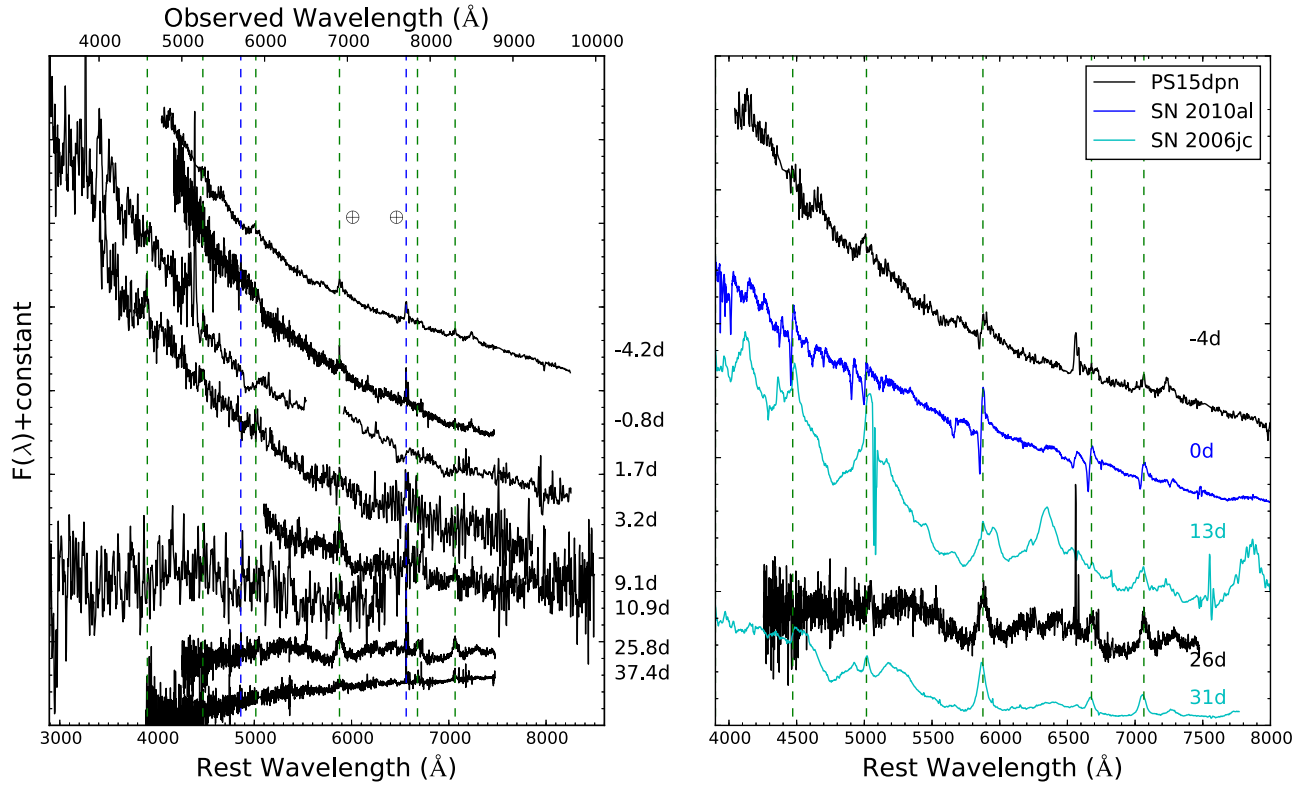

Figure 4. Spectra of PS15dpn from the combined GMOS, PESSTO, and SNIFS campaigns. The vertical dashed green lines refer to He I and He II lines, while the blue (only shown on left) line refers to Hα and Hβ. The right panel refers to rest-frame days after peak.

bursts (LGRBs). Figure 1 shows that if an energetic type Ic SN accompanies such a GRB event then it would be an unambiguous, bright transient in our survey. We do not find such an object, but caution that we surveyed a maximum of 26.5% of the total LIGO probability region. Our results are encouraging for future searches for the counterparts of NS–NS mergers within about 100 Mpc where the predicted optical and near infrared counterparts are within reach.

PS1 and ATLAS are supported by NASA grants NNX08AR22G, NNX12AR65G, NNX14AM74G, and NNX12AR55G. This work is based on data from: ESO as part of PESSTO (188.D-3003, 191.D-0935), Gemini Program GN-2016A-Q-36, GN-2015B-Q-4, the UH 2.2 m, and the NASA/ESA *Hubble Space Telescope* program 14484. We thank Gemini and *HST* for Director's Discretionary time. We acknowledge EU/FP7-ERC grants [291222,307260,320360,615929], a Weizmann-UK Making Connections Grant, a STFC Ernest Rutherford Fellowship (K.M.), and a Sofia Kovalevskaja Award from the Alexander von Humboldt Foundation (T.W.C.). PS1 surveys acknowledge the PS1SC: University of Hawaii, MPIA Heidelberg, MPE Garching, Johns Hopkins University, Durham University, University of Edinburgh, Queen's University Belfast, Harvard-Smithsonian CfA, LCOGT, NCU Taiwan, STScI, University of Maryland, Eotvos Lorand University, Los Alamos National Laboratory, and NSF grant No. AST-1238877.

REFERENCES

Abadie, J., Abbott, B. P., Abbott, R., et al. 2010, CQGra, 27, 173001
Abbott, B. P., Abbott, R., Abbott, T. D., et al. 2016a, ApJL, 818, L22
Abbott, B. P., Abbott, R., Abbott, T. D., et al. 2016b, PhRvL, 116, 241103
Abbott, B. P., Abbott, R., Abbott, T. D., et al. 2016c, ApJL, 826, L13
Abbott, B. P., Abbott, R., Abbott, T. D., et al. 2016d, PhRvL, 116, 061102
Barnes, J., & Kasen, D. 2013, ApJ, 775, 18
Berger, E., Leibler, C. N., Chornock, R., et al. 2013, ApJ, 779, 18
Castro-Tirado, P., Caballero-Garcia, E., et al. 2016, GCN, 19258, http://gcn.gsfc.nasa.gov/gcn3/19258.gcn3
Cenko, S. B., Cao, Y., Ferretti, R., et al. 2016a, GCN, 18762, http://gcn.gsfc.nasa.gov/gcn3/18762.gcn3
Cenko, S. B., Kasliwal, M., Singer, L., et al. 2016b, GCN, 18848, http://gcn.gsfc.nasa.gov/gcn3/18848.gcn3
Chambers, K. C., Chen, T., Smartt, S., et al. 2016, GCN, 18811, http://gcn.gsfc.nasa.gov/gcn3/18811.gcn3
Connaughton, V., Burns, E., Goldstein, A., et al. 2016, ApJL, 826, L6
Copperwheat, C. M., & Steele, I. 2016a, GCN, 18791, http://gcn.gsfc.nasa.gov/gcn3/18791.gcn3
Copperwheat, C. M., & Steele, I. 2016b, GCN, 18807, http://gcn.gsfc.nasa.gov/gcn3/18807.gcn3
Corsi, A., & Palliyaguru, N. 2016, GCN, 18873, http://gcn.gsfc.nasa.gov/gcn3/18873.gcn3
Coughlin, M. W., & Stubbs, C. W. 2016, ExA, in press (arXiv:1604.05205)
Crowther, P. A., Barnard, R., Carpano, S., et al. 2010, MNRAS, 403, L41
D'Avanzo, P., Melandri, A., et al. 2016, GCN, 18868, http://gcn.gsfc.nasa.gov/gcn3/18868.gcn3
Foley, R. J., Smith, N., Ganeshalingam, M., et al. 2007, ApJL, 657, L105
Frohmaier, C., Dimitriadis, G., Firth, R., et al. 2016, GCN, 18806, http://gcn.gsfc.nasa.gov/gcn3/18806.gcn3
Galama, T. J., Vreeswijk, P. M., van Paradijs, J., et al. 1998, Natur, 395, 670
Gorbikov, E., Gal-Yam, A., Ofek, E. O., et al. 2014, MNRAS, 443, 671
Greiner, J., Burgess, J. M., Savchenko, V., & Yu, H.-F. 2016, ApJL, 827, L38
Inserra, C., Smartt, S. J., Gall, E. E. E., et al. 2016, arXiv:1604.01226
Inserra, C., Smartt, S. J., Jerkstrand, A., et al. 2013, ApJ, 770, 128
Kaiser, N., Burgett, W., Chambers, K., et al. 2010, Proc. SPIE, 7733, 77330E
Kasen, D., Fernández, R., & Metzger, B. D. 2015, MNRAS, 450, 1777
Lipunov, V., Gorbovskoy, E., Tyurina, N., et al. 2016, GCN, 18804, http://gcn.gsfc.nasa.gov/gcn3/18804.gcn3
Loeb, A. 2016, ApJL, 819, L21
Lombriser, L., & Taylor, A. 2016, JCAP, 3, 031
Magnier, E. A., Schlafly, E., Finkbeiner, D., et al. 2013, ApJS, 205, 20
Martynov, D. V., Hall, E. D., Abbott, B. P., et al. 2016, PhRvD, 93, 112004
Palazzi, P., Cappellaro, E., et al. 2016, GCN, 19145, http://gcn.gsfc.nasa.gov/gcn3/19145.gcn3

Pan, Y.-C., Downing, S., Foley, R. J., et al. 2016, ATel, 8506
Pastorello, A., Benetti, S., Brown, P. J., et al. 2015, MNRAS, 449, 1921
Pastorello, A., Mattila, S., Zampieri, L., et al. 2008, MNRAS, 389, 113
Pastorello, A., Smartt, S. J., Mattila, S., et al. 2007, Natur, 447, 829
Patat, F., Cappellaro, E., Danziger, J., et al. 2001, ApJ, 555, 900
Perna, R., Lazzati, D., & Giacomazzo, B. 2016, ApJL, 821, L18
Prestwich, A. H., Kilgard, R., Crowther, P. A., et al. 2007, ApJL, 669, L21
Schlafly, E. F., Finkbeiner, D. P., Jurić, M., et al. 2012, ApJ, 756, 158
Singer, L. P., & Price, L. R. 2016, PhRvD, 93, 024013
Smartt, S. J., Chambers, K. C., Smith, K. W., et al. 2016, MNRAS, in press (arXiv:1602.04156)
Smartt, S. J., Valenti, S., Fraser, M., et al. 2015, A&A, 579, A40
Soderberg, A. M., Chakraborti, S., Pignata, G., et al. 2010, Natur, 463, 513
Tanaka, M., & Hotokezaka, K. 2013, ApJ, 775, 113
Tanaka, M., Hotokezaka, K., Kyutoku, K., et al. 2014, ApJ, 780, 31
The LIGO Scientific Collaboration and the Virgo Collaboration 2016a, GCN, 18850, http://gcn.gsfc.nasa.gov/gcn3/18850.gcn3
The LIGO Scientific Collaboration and the Virgo Collaboration 2016b, https://dcc.ligo.org/LIGO-P1600088/main/public
Tonry, J., Denneau, L., Stalder, B., et al. 2016, ATel, 8680
Tonry, J. L. 2011, PASP, 123, 58
Tonry, J. L., Stubbs, C. W., Lykke, K. R., et al. 2012, ApJ, 750, 99
Woosley, S. E. 2016, ApJL, 824, L10
Wright, D. E., Smartt, S. J., Smith, K. W., et al. 2015, MNRAS, 449, 451